Society for Endocrinology
JOURNAL OF ENDOCRINOLOGY

The role of *Mif* deficiency in glucocorticoid-mediated adiposity in fructose-fed mice

Journal:	*Journal of Endocrinology*
Manuscript ID	Draft
Manuscript Type:	Research Paper
Date Submitted by the Author:	n/a
Complete List of Authors:	Gligorovska, Ljupka; Univerzitet u Beogradu Institut za bioloska istrazivanja Sinisa Stankovic, Department of Biochemistry Bursac, Biljana; Univerzitet u Beogradu Institut za bioloska istrazivanja Sinisa Stankovic, Department of Biochemistry Kovacevic, Sanja; Univerzitet u Beogradu Institut za bioloska istrazivanja Sinisa Stankovic, Department of Biochemistry Velickovic, Natasa; Univerzitet u Beogradu Institut za bioloska istrazivanja Sinisa Stankovic, Department of Biochemistry Matić, Gordana; Institute for Biological Research "Siniša Stanković", Department of Biochemistry Djordjevic, Ana; Instiute for Biological Research "Sinisa Stankovic", University of Belgrade, Department of Biochemistry
Keywords:	macrophage migration inhibitory factor, glucocorticoids, visceral adipose tissue, lipid metabolism, Insulin Resistance

UNIVERSITY OF BELGRADE
INSTITUTE FOR BIOLOGICAL RESEARCH "SINIŠA STANKOVIĆ"
Department of Biochemistry

✉ 142 Despot Stefan Blvd., 11060 Belgrade, Serbia ☎ +381/11/2078318 🖷 +381/11/2761433

Journal of Endocrinology Belgrade, May 31, 2018

Co-Editors-In-Chief
Prof. Dr. S. Andrikopoulos
Prof. Dr. C. Farquharson

Dear Professors,

Please find attached our manuscript, entitled **'The role of Mif deficiency in glucocorticoid-mediated adiposity in fructose-fed mice'** by Ljupka Gligorovska, Biljana Bursać, Sanja Kovačević, Nataša Veličković, Gordana Matić and Ana Djordjevic, which we would like to be considered for publication in **Journal of Endocrinology.**

We believe that the results of this study will contribute to the better understanding of crosstalk between glucocorticoids and insulin in macrophage migration inhibitory factor (MIF) *knock-out* mice, which exhibit disturbed insulin resistance in the absence of this proinflammatory cytokine. The metabolic perturbations observed in fructose-fed *Mif* deficient mice are most likely a result of enhanced visceral adipose tissue glucocorticoid signaling in the hyperinsulinemic setting, pointing out the possibility of a regulatory loop between MIF and glucocorticoids under the conditions of caloric overload.

All animal procedures were in compliance with the EEC Directive (2010/63/EU) on the protection of animals used for experimental and other scientific purposes, and were approved by the Ethical Committee for the Use of Laboratory Animals of the Institute for Biological Research "Siniša Stanković", University of Belgrade.

All authors have substantially contributed to the work, participated in the writing of the manuscript and approved the submitted version. No part of the work has been published before, except in the abstract form. The work has not been and will not be submitted for publication elsewhere until the editorial board has decided whether to publish the article. We hope that you will find that the topics covered by our study will be interesting for the readers of **Journal of Endocrinology.**

Sincerely yours,

Ana Djordjevic, PhD
Department of Biochemistry,
Institute for Biological Research "Siniša Stanković",
142 Despot Stefan Blvd.,
11000 Belgrade, Serbia
Phone: +381 11 207 83 18; Fax:+381 11 276 14 33
e-mail: djordjevica@ibiss.bg.ac.rs

The role of *Mif* deficiency in glucocorticoid-mediated adiposity in fructose-fed mice

Ljupka Gligorovska*, Biljana Bursać, Sanja Kovačević, Nataša Veličković, Gordana Matić, Ana Djordjevic§

Department of Biochemistry, Institute for Biological Research "Siniša Stanković", University of Belgrade, 142 Despot Stefan Blvd., 11000 Belgrade, Serbia

§ Corresponding author:
Ana Djordjevic, PhD
Department of Biochemistry, Institute for Biological Research "Siniša Stanković",
142 Despot Stefan Blvd., 11000 Belgrade, Serbia
Phone: +381 11 207 83 18; Fax: +381 11 276 14 33
e-mail: djordjevica@ibiss.bg.ac.rs

Short title: MIF and fructose-related adiposity

Key words: macrophage migration inhibitory factor; insulin resistance; fructose; glucocorticoids; visceral adipose tissue; lipid metabolism

Word count: 4971

Abstract

The macrophage migration inhibitory factor (MIF) is a pro-inflammatory cytokine involved in metabolic inflammation, regulation of energy metabolism and glucocorticoid action. Chronic low-grade inflammation may be caused by excess fructose intake, which contributes to intra-abdominal adiposity and dysfunction of the adipose tissue. We hypothesized that the effects of MIF on lipid metabolism in the visceral adipose tissue, after fructose consumption, are mediated by glucocorticoids as potent regulators of energy metabolism. We analyzed physiological and biochemical parameters, adipose tissue histology, insulin sensitivity and lipid metabolism in *wild type* and *Mif* deficient ($MIF^{-/-}$) C57Bl/6J mice consuming 20% fructose solution for 9 weeks. Glucocorticoid prereceptor metabolism and glucocorticoid receptor (GR) protein level were examined in VAT, together with the expression of glucocorticoid-target genes involved in lipid metabolism. We also analyzed the expression of key transcriptional regulators involved in adipogenesis and lipogenesis: peroxisome proliferator activated receptor gamma (PPARG) and sterol regulatory element-binding protein 1c (SREBP1c). Disturbed insulin sensitivity was observed in all $MIF^{-/-}$ mice, regardless of the diet regime. Mice on fructose diet had increased energy intake, but increased visceral adiposity and enlarged adipocytes were observed only in fructose-fed $MIF^{-/-}$ mice. Enhanced glucocorticoid signaling, together with induced expression of all examined lipogenic genes and accumulation of PPARG and SREBP1c, were observed in the same animals. In conclusion, the results showed that dietary fructose overload led to increased visceral adiposity through activation of GR-regulated lipogenic genes, but only in the absence of MIF, which set the state of hyperinsulinemia and insulin resistance.

1. Introduction

The rate of fructose consumption has been increasing worldwide and is considered to be a contributing factor to the rising prevalence of obesity and metabolic disturbances. There are evidence from human and animal studies supporting the ability of high-fructose diet to upregulate lipid metabolism leading to dyslipidemia, insulin resistance and type 2 diabetes (T2D) (Basciano *et al.* 2005; Tappy & Le 2010). Excess fructose intake can also contribute to intra-abdominal adiposity and dysfunction of the adipose tissue, resulting in the infiltration of immune cells and development of chronic low-grade inflammation (Monteiro & Azevedo 2010).

Macrophage migration inhibitory factor (MIF) is a pleiotropic ubiquitously expressed cytokine that regulates pro-inflammatory response and is associated with numerous inflammatory and autoimmune diseases including T2D and obesity (Cvetkovic *et al.* 2005). A growing body of evidence indicates that MIF has a role in energy metabolism in the adipose tissue and liver, since its expression in these tissues is regulated by glucose and insulin (Sakaue *et al.* 1999; Morrison & Kleemann 2015). *Mif* deletion may contribute to development of systemic insulin resistance through deregulation of glucose metabolism (Atsumi *et al.* 2007; Nikolic *et al.* 2013; Saksida *et al.* 2013). However, the data are still inconclusive, since there are studies reporting that *Mif knock-out* mice display improved insulin sensitivity and glucose tolerance (Verschuren *et al.* 2009; Kleemann & Bucala 2010).

Although MIF synthesis and secretion could be upregulated by the glucocorticoid hormones (GCs), MIF acts as the counter-regulator of GC anti-inflammatory action to control the magnitude of the immune response (Calandra & Bucala 1997). Systemic hypercortisolemia and overexpression of enzymes converting inactive forms of GCs to active ones, 11beta-hydroxysteroid dehydrogenase type-1 (11BHSD1) and hexose-6-phosphate dehydrogenase (H6PDH), were previously associated with increased accumulation of visceral

adipose tissue (VAT) (Seckl *et al.* 2004; Mariniello *et al.* 2006). GCs affect carbohydrate and lipid metabolism through hormone-dependent transcription regulator, glucocorticoid receptor (GR) (Peckett *et al.* 2011). Depending on nutritional and energy state, GCs can dually affect lipid metabolism. These effects can be opposite to insulin action, since GR directly regulates transcription of lipolytic enzymes, adipose tissue triglyceride lipase (ATGL) and hormone-sensitive lipase (HSL) (Lee *et al.* 2014). On the other hand, when insulin levels are high, GCs and insulin synergistically increase expression of lipogenic genes, including lipoprotein lipase (*Lpl*), fatty acid synthase (*Fas*), acetyl-CoA carboxylase (*Acc*) and phosphoenolpyruvate carboxykinase (*Pepck*) (Chakravarty *et al.* 2005; Campbell *et al.* 2011; Peckett *et al.* 2011). Besides GR, a number of insulin-regulated transcriptional factors is engaged in lipid metabolism and adipose tissue development. The examples are sterol regulatory element binding protein 1c (SREBP1c), responsible for triglyceride biosynthesis, as well as peroxisome proliferator-activated receptor gamma (PPARG) involved in adipocyte differentiation (Rosen & Spiegelman 2001; Eberlé *et al.* 2004).

Circulating MIF levels and intracellular GCs are shown to be elevated in obese subjects; however their role and interaction in changes of lipid metabolism and insulin resistance induced by high-fructose diet remains elusive. The aim of this study was to investigate whether genetic deletion of *Mif* results in GC-mediated disturbances of lipid and glucose metabolism in VAT of fructose-fed mice. We analyzed the effects of 20% fructose diet for 9-weeks on energy intake, physiological parameters, VAT histology, biochemical parameters of insulin sensitivity and lipid metabolism, p38 kinase level and GR signaling, as well as on the expression of GC-target genes involved in lipolysis and lipogenesis in the VAT of male $MIF^{-/-}$ mice and their WT C57BL/6J counterparts.

2. Materials and methods

2.1. Animals and treatment

During nine weeks, homozygous male MIF$^{-/-}$ mice (background: C57BL/6J) (Fingerle-Rowson *et al.* 2003) and WT C57BL/6J were kept in a temperature-controlled room (22 ± 2°C) with a 12h light/dark cycle (lights on at 07:00 h) in the Animal Facility at the Institute for Biological Research "Siniša Stanković". The 2 months old animals were divided into 4 experimental groups (n = 12 animals per group): WT and MIF$^{-/-}$ mice had standard diet (commercial chow and drinking water available *ad libitum*), while WT and MIF$^{-/-}$ mice on fructose rich diet had *ad libitum* access to commercial chow and to 20% fructose solution instead of drinking water (WT FrD and MIF$^{-/-}$ FrD, respectively). The detailed composition of the diet was described previously (Veličković *et al.* 2013). The animals were housed 4 per cage, and daily food and fluid intake were measured during 9 weeks. Body mass was measured weekly. Energy intake for mice on standard diet was calculated as food weight (g) × 11 kJ, while energy intake for mice on fructose diet was calculated as sum of calories ingested as food and fructose solution [food weight (g) × 11 kJ + fructose intake (ml) × 1.72 kJ × 2]. All animal procedures were in compliance with the EEC Directive 2010/63/EU on the protection of animals used for experimental and other scientific purposes, and were approved by the Ethical Committee for the Use of Laboratory Animals of the Institute for Biological Research "Siniša Stanković", University of Belgrade.

2.2.1. Intraperitoneal glucose (IP-GTT) and insulin tolerance tests (IP-ITT)

IP-GTT was performed 3 days before the end of the treatment. Mice were fasted overnight and glucose challenge was given intraperitoneally (2 g/kg) without anesthesia in order to avoid the effect of anesthetic on glucose level and kinetics of glucose disposal. In order to determine glucose concentration, blood samples were taken from the tip of the tail at

0, 15, 30, 60, 90 and 120 min after injection. For IP-ITT, mice were fasted for 4 hours prior to the test. Blood glucose was measured at 0, 15, 30, 60, 90 and 120 min after the insulin injection (0.75 IU/kg). The concentration of glucose in the blood was measured by Accu-Chek Active® strips (F. Hoffmann-La Roche AG, Basel, Switzerland). The area under the concentration vs. time curve (AUC glucose 0-120 min, mmol/l vs. min) was calculated by the trapezoidal rule.

2.2.2. Blood sample collection and determination of plasma parameters

Mice were sacrificed by rapid decapitation after overnight fasting. Trunk blood was collected into EDTA containing tubes. Blood glucose and tryglicerides were measured by Accutrend® strips (F. Hoffmann-La Roche AG, Basel, Switzerland). Plasma was prepared by low speed centrifugation (1600 g/10 min) and stored at -20°C for subsequent processing. Free fatty acids (FFA) were determined by the Semi-auto Chemistry Analyzer (Rayito 1904C) using Randox NEFA kit (Randox Laboratories Ltd, Crumlin, UK). Adipose tissue corticosterone (CORT) was assessed using Corticosterone High Sensitivity EIA kit according to manufacturer's instructions (Immunodiagnostic Systems LTD, Tyne and Wear, UK). Insulin concentration was determined by RIA method, using mouse insulin standards (INEP, Belgrade, Serbia). The assay sensitivity was 0.6 mIU/l and intra-assay coefficient of variation was 5.24 %.

2.3. Isolation of visceral adipose tissue

VAT (consisting of gonadal, retroperitonel and perirenal depot) was excised, washed by 0.9% NaCl solution, weight and frozen in liquid nitrogen. For histological analysis, part of the tissue was fixed in 10% neutral formalin for 24 h, dehydrated in ethanol gradient, cleared in xylene and embedded in paraffin.

152 *2.4. Histological analysis of VAT*

153 VAT blocks were sectioned at 10 μm thickness and stained with hematoxylin-eosin.
154 Morphometric analysis was carried on workstation comprising of microscope (Olympus, BX-
155 51, Tokyo, Japan) equipped with a charge-coupled device (CCD) video camera (PixeLINK,
156 Ottawa, Canada). The system was controlled by the newCAST software package
157 (Visiopharm Integrator System, version 3.2.7.0, Visiopharm, Denmark). Images were
158 analyzed by Adiposoft software (Galarraga *et al.* 2012). The cell diameter and sectional area
159 were measured using 3 images per section (20x magnification), 3 sections per animal and 5
160 animals per group.

161

162 *2.5.1. RNA extraction and Reverse Transcription*

163 VAT total RNA was isolated using TRIzol® (AmBion, Life Technologies, Carlsbad,
164 USA). After homogenization, samples were centrifuged at 12000 g for 15 min at 4°C. RNA
165 was precipitated with isopropanol. Quantitative and qualitative evaluation of the isolated
166 RNA was performed spectrophotometrically (OD 260/280 > 1.8 was considered satisfactory)
167 and on 2% agarose gel. Reverse transcription was performed using a High-Capacity cDNA
168 Reverse Transcription Kit (Applied Biosystems, Foster City, USA) according to
169 manufacturer's instructions and the cDNAs were stored at -70°C until use.

170

171 *2.5.2. Real-time PCR*

172 The expression of genes was analyzed using Power SYBR® Green PCR Master Mix.
173 Specific primers (Applied Biosystems, Foster City, USA) were used to selectively amplify
174 *Hsl*: F 5'-GGC TCA CAG TTA CCA TCT CAC C-3', R 5'-GAG TAC CTT GCT GTC CTG
175 TCC-3'; *Atgl*: F 5'-AAC ACC AGC ATC CAG TTC AA-3', R 5'-GGT TCA GTA GGC
176 CAT TCC TC-3'; *Pepck*: F 5'-AAC TGT TGG CTG GCT CTC-3', R 5'-GAA CCT GGC

GTT GAA TGC-3'; *Lpl*: F 5'-TTC CAG CCA GGA TGC AAC A-3', R 5'-GGT CCA CGT CTC CGA GTC C-3'; *Acc*: F 5'-GAG AGG GGT CAA GTC CTT CC-3', R 5'-CTG CTG CCG TCA TAA GAC AA-3'; *Fas*: F 5'-TTG CTG GCA CTA CAG AAT GC-3', R 5'-AAC AGC CTC AGA GCG ACA AT-3'. Normalization of cDNA in each sample was performed using hypoxanthine guanine phosphoribosyl transferase (*Hprt*) as endogenous control (F 5'-TCC TCC TCA GAC CGC TTT T-3', R 5'-CCT GGT TCA TCA TCG CTA ATC-3'). All reactions were performed in triplicate in 25 µl volume containing 20 ng of cDNA template using QuantStudio™ 3 (Applied Biosystems, Foster City, USA). Thermal cycling conditions were 2 min incubation at 50 °C, 10 min at 95 °C followed by 60 cycles of 95 °C for 15 s and 60 °C for 60 s. Melting curve analyses were performed at the end of every experiment to confirm formation of a single PCR product. Relative quantification of gene expression was performed using the comparative $2^{-\Delta Ct}$ method, where ΔCt represent the difference between Ct value of target gene and the endogenous control. The results were analyzed by QuantStudio™ Design and Analysis Software v1.4.0 (Applied Biosystems, Foster City, USA) with a confidence level of 95% ($p \leq 0.05$).

2.6.1. Sample preparation

For the preparation of VAT total protein fraction, TRIzol® was used according to the manufacturers instruction. After aqueous phase separation for RNA precipitation, the remaining organic phase was centrifuged at 2 000 g for 5 min at 4°C after adding ethanol. Protein fraction was precipitated from phenol-ethanol supernatant, using acetone and centrifuged at 12000 g for 10 min at 4°C. The protein pellets were dispersed in 0.3 M guanidine hydrochloride in 95% ethanol with 2.5% glycerol by sonication on ice and washed in 0.3 M guanidine hydrochloride in 95% ethanol with 2.5% glycerol. After sedimenting the protein by centrifugation at 8 000 g for 5 min at 4°C, pellets were dispersed in the lysis buffer

containing 2.5 mM Tris-HCl pH 6.8, 2% sodium dodecyl sulfate (SDS), 10% glycerol and 50 mM DTT. All samples were stored at -70°C until use.

2.6.2. Western blot analysis

Proteins concentration was measured using Lowry method (Lowry *et al.* 1951) and 60 µg of proteins was subjected to electrophoresis on 7.5% SDS-PAGE. After transfer to PVDF membrane (Immobilon-FL membrane, Millipore, USA), using a Transblot system (Bio-Rad Laboratories, Hercules, USA), the unbound sites were blocked (1 h with 2% non-fat dry milk) and the membranes were probed with specific primary rabbit polyclonal antibodies for anti-phospho-p38 Tyr 182 (1:750) (sc-7975-R, Santa Cruz Biotechnology, Dallas, USA), anti-p38 MAPK (1:500) (sc-535, Santa Cruz Biotechnology, Dallas, USA), anti-GR (1:500) (sc-8992, Santa Cruz Biotechnology, Dallas, USA), anti-11BHSD1 (1:1000) (ab393364, Abcam, Cambridge, UK), anti-H6PDH (1:1000) (sc-67394, Santa Cruz Biotechnology, Dallas, USA), anti-SREBP1c (1:500) (sc-366, Santa Cruz Biotechnology, Dallas, USA) and mouse monoclonal anti-PPARG (1:1000) (sc-7273, Santa Cruz Biotechnology, Dallas, USA). Monoclonal mouse anti-B-actin antibody (1:10000) (AC-15, Sigma-Aldrich, St. Louis, USA) was used as a loading control. Blots were developed with secondary ECL anti-rabbit IgG HRP-linked whole antibody (1:10000) (Amersham Pharmacia Biotech, UK) or with anti-mouse IgG HRP-linked whole antibody (1:20000) (ab97046, Abcam, Cambridge, UK). Signal was developed using enhanced chemiluminescence (ECL) and densitometry of protein bands on X-ray films (Kodak, Rochester, USA) was performed by Image J software (NIH, Bethesda, USA).

227 *2.7. Statistical analyses*

228 Physiological, biochemical and histological data are presented as means ± SD, while
229 data from Western blot and qPCR are presented as means ± SEM. To determine the effects of
230 *Mif* deficiency and fructose diet, as well as their interaction, two-way ANOVA followed by
231 *post-hoc* Tukey test was used. A probability level less than 0.05 was considered statistically
232 significant. Statistical analyses were performed by Statistica 10 Software (Stat Soft. Inc.,
233 Tulsa, USA).

234

235 **3. Results**

236 *3.1. Physiological measurements*

237 Fructose-fed WT mice had decreased food and increased liquid intake compared to
238 the WT ones ($p < 0.001$), while $MIF^{-/-}$ mice on fructose diet ate less food and drank more
239 liquid than WT and $MIF^{-/-}$ animals (Table 1, $p < 0.001$). However, $MIF^{-/-}$ animals consumed
240 less liquid in comparison to their counterparts on the same diet ($p < 0.001$). WT mice on
241 fructose diet had increased energy intake compared to the WT mice on standard diet ($p <$
242 0.001), while fructose-fed $MIF^{-/-}$ consumed more energy than both WT and $MIF^{-/-}$ animals (p
243 < 0.001), but had lower energy intake when compared to WT mice on fructose diet ($p <$
244 0.05).

245 Despite increased energy intake, body mass and weight gain of fructose-fed mice was
246 not significantly different from the animals on the standard diet (Figure 1A). Interestingly,
247 mass of VAT was higher in *Mif* deficient mice in comparison to WT animals (Figure 1B, $p <$
248 0.05), while fructose-fed $MIF^{-/-}$ mice had significantly more VAT than both WT ($p < 0.001$)
249 and WT mice consuming fructose ($p < 0.01$). However, VAT-to-body mass ratio, taken as an
250 index of visceral adiposity, was significantly increased only in *Mif* deficient mice on fructose

diet in comparison to WT groups on standard and fructose diet (Figure 1C, $p < 0.001$ and $p < 0.01$, respectively), as well as to MIF$^{-/-}$ mice on standard diet ($p < 0.05$).

3.2. Measurements of plasma triglycerides, FFA and insulin sensitivity parameters

Both plasma triglycerides and FFA were the same in all expreimental groups (see Table 1).

As shown in Table 2, MIF$^{-/-}$ mice had significantly higher fasting glucose than WT animals ($p < 0.05$), while in fructose-fed MIF$^{-/-}$ mice glucose level was higher only in comparison to WT mice consuming fructose ($p < 0.01$). Increased insulin was present in MIF$^{-/-}$ mice in comparison to WT ($p < 0.05$), while MIF$^{-/-}$ mice on fructose diet had higher insulin level than their WT counterparts on both standard ($p < 0.01$) and fructose diet ($p < 0.05$).

Insulin sensitivity was estimated by IP-GTT and IP-ITT tests and the results showed that both fructose diet and *Mif* deficiency contributed to its disturbance (Figure 2). Namely, an increase of AUC value was detected in MIF$^{-/-}$ mice compared to WT counterparts (Table 2 and Figure 2A, $p < 0.001$), while this value was significantly higher in MIF$^{-/-}$ mice on fructose diet in comparison to MIF$^{-/-}$ mice on normal diet ($p < 0.05$) and to WT mice consuming fructose ($p < 0.001$). Similarly, the AUC values during ITT were significantly increased in MIF$^{-/-}$ group in respect to WT animals ($p < 0.001$) and in MIF$^{-/-}$ mice on fructose diet in respect to both WT and fructose-fed WT mice ($p < 0.001$).

3.3. Histological and morphometrical analysis of VAT

VAT histological analysis revealed large adipocytes in MIF$^{-/-}$ mice on fructose diet (Figure 1D-G). Morphometrical analysis showed that both adipocyte cell diameter and area (Figure 1H and I) were significantly increased in fructose-fed MIF$^{-/-}$ mice in comparison to

both WT mice on standard ($p < 0.01$) and fructose diet ($p < 0.05$), as well as in comparison to *Mif* deficient mice on standard diet ($p < 0.05$).

3.4. Signaling pathway of p38 kinase in VAT

Fructose and *Mif* deficiency, alone or in combination, induced changes in p38 kinase in VAT. Elevation of total p38 protein level was observed in all experimental groups in respect to WT animals (Figure 3, $p < 0.001$). Also, $MIF^{-/-}$ animals on fructose diet had elevated total p38 protein level compared to their WT counterparts on the same dietary regime ($p < 0.001$), while the level of this protein was decreased in comparison to $MIF^{-/-}$ animals on standard diet ($p < 0.001$). On the other hand, a significant increase of phosphorylated p38 was observed in all animals on fructose diet compared to the WT ($p < 0.05$), as well as in fructose-fed $MIF^{-/-}$ mice in comparison to $MIF^{-/-}$ animals on standard diet ($p < 0.05$). Finaly, the ratio of phosphorylated to total p38 level, taken as an indicator of the enzyme activity, was higher in WT animals on fructose diet compared to the same animals on standard diet ($p < 0.05$), but also in $MIF^{-/-}$ mice on fructose diet compared to $MIF^{-/-}$ mice on standard diet ($p < 0.05$).

3.5. Glucocorticoid prereceptor metabolism and signaling

VAT glucocorticoid signaling was examined at the level of prereceptor metabolism (protein levels of 11BHSD1 and H6PDH enzymes and intracellular level of CORT), and at GR protein level. As shown in Figure 4A and B, an increase of 11BHSD1 and H6PDH was observed in $MIF^{-/-}$ animals on fructose diet in respect to WT ($p < 0.001$ and $p < 0.01$, respectively) and $MIF^{-/-}$ mice on standard diet ($p < 0.01$).

In line with enchanced prereceptor metabolism, increased VAT CORT (Figure 4C) was observed in fructose-fed $MIF^{-/-}$ mice in comparison to both normally fed and fructose-fed

300 WT mice ($p < 0.05$), as well as in comparison to standard-fed MIF$^{-/-}$ animals ($p < 0.01$). In
301 addition, GR protein level was elevated only in fructose-fed MIF$^{-/-}$ mice compared to WT
302 group (Figure 4D, $p < 0.05$).
303
304 *3.6. Lipid metabolism in VAT*
305 The results showed changes in the expression of GR-target genes involved in VAT
306 lipid metabolism in fructose-fed MIF$^{-/-}$ mice (Figure 5). Namely, the increase of *Fas* was
307 detected in VAT of these animals in comparison to WT animals irrespective of the diet ($p <$
308 0.01), and also in comparison to MIF$^{-/-}$ mice on standard diet ($p < 0.05$). *Acc* mRNA level
309 was also increased in MIF$^{-/-}$ mice in comparison to WT ($p < 0.001$), fructose-fed WT ($p <$
310 0.01) and normally fed MIF$^{-/-}$ ($p < 0.05$) mice. *Pepck* mRNA level was significantly increased
311 in *Mif* deficient mice on fructose diet in comparison to all other experimental groups ($p <$
312 0.001). However, mRNA level for the main lipolytic enzyme *Atgl* was also significantly
313 higher in fructose-fed MIF$^{-/-}$ mice compared to both WT groups (standard diet: $p < 0.001$;
314 fructose diet: $p < 0.01$), as well as compared to normally fed MIF$^{-/-}$ ($p < 0.01$). Interestingly,
315 the level of *Hsl* mRNA was unchanged (Figure 5). In addition, *Lpl* mRNA was increased in
316 fructose-fed WT mice, and in both MIF$^{-/-}$ mice on standard and fructose diet in comparison to
317 the WT animals ($p < 0.05$, $p < 0.01$, $p < 0.001$, respectively), but also in MIF$^{-/-}$ mice
318 compared to fructose-fed MIF$^{-/-}$ animals ($p < 0.01$).
319 Protein levels of key transcriptional regulators involved in adipogenesis and
320 lipogenesis, PPARG and SREBP1c, were determined in VAT total protein extract (Figure 6).
321 PPARG was increased in MIF$^{-/-}$ mice on fructose diet, as compared to WT and MIF$^{-/-}$ animals
322 ($p < 0.05$), while SREBP1c protein level was significantly increased in the same group of
323 animals compared to WT ($p < 0.001$) and both fructose-fed WT and MIF$^{-/-}$ ($p < 0.01$).
324

4. Discussion

Many studies have indicated the importance of MIF for glucose homeostasis, however, its role in metabolic disturbances is less clear. In our study, *Mif* deficient mice were hyperglycemic, hyperinsulinemic and had impaired insulin sensitivity. On the other hand, energy-rich fructose diet in $MIF^{-/-}$ mice resulted in increased visceral adiposity, underlaid by stimulated expression of lipogenic genes and the activation of key transcriptional regulators of VAT adipogenesis and lipogenesis, PPARG and SREBP1c. These metabolic perturbations in *Mif* deficient mice are most likely a result of enhanced VAT glucocorticoid signaling in the hyperinsulinemic setting, pointing out the possibility of a regulatory loop between MIF and GCs under the conditions of caloric overload induced by high fructose diet.

Increasing evidence suggests that MIF is released by the adipose tissue in obesity and that it is also involved in metabolic and inflammatory processes underlying the development of T2D. In our study the hallmarks of systemic insulin resistance were observed in all $MIF^{-/-}$ mice, regardless of the diet regime and adiposity. Namely, all *Mif* deficient mice exhibited hyperglycemia, hyperinsulinemia and impaired glucose and insulin tolerance (Table 2, Figure 2). Although some studies have reported that deletion of *Mif* improved insulin sensitivity and glucose tolerance (Verschuren *et al.* 2009; Kleemann & Bucala 2010), the others have shown that $MIF^{-/-}$ mice became obese and insulin resistant (Serre-Beinier *et al.* 2010; Nikolic *et al.* 2013; Saksida *et al.* 2013). One of the possible reasons for such a discrepancy could be found in the age of experimental animals, since it was shown that mature adult mice, as those used in the present study, are more prone to insulin resistance and obesity than the young ones (Serre-Beinier *et al.* 2010). Besides regulating glucose metabolism, MIF may also be linked to disturbed energy metabolism under caloric overload (Finucane *et al.* 2014; Kim *et al.* 2015). Thus one study reported that *Mif* deficiency in C57BL/6 mice kept on high fat diet promotes weight gain and has detrimental effects on glucose tolerance, while adipose tissue

inflammation was reduced in the absence of *Mif* (Heinrichs *et al.* 2014). The present study demonstrated increased visceral adiposity and adipocyte hypertrophy only in MIF$^{-/-}$ mice on fructose diet (Figure 1), which points out the importance of MIF in the development of obesity induced by fructose feeding.

The other important hormonal factors interfering with MIF activity are the GCs. It was previously established that their physiological concentrations can alter MIF expression and secretion, but there are also evidence showing *vice versa*. Namely, MIF can limit GCs effects, most likely through p38 phosphorylation, while the absence of endogenous MIF is associated with increased sensitivity to GCs through decreased phosphorylation of p38 MAPK (Calandra *et al.* 1995; Aeberli *et al.* 2006a, b). Proinflammatory p38 kinase is activated by oxidative stress and inflammation in 3T3-L1 cells and human adipocytes (Merkel *et al.* 2002; Chuang *et al.* 2010; Vazquez Prieto *et al.* 2015; Cheng *et al.* 2017), and fructose diet is known to enhance the production of proinflammatory cytokines and oxidative stress mediators in rodent visceral adipose tissue (Kovačević *et al.* 2016; Pektas *et al.* 2016). Our results showed that fructose diet indeed led to elevation in both total and phospho p38 protein levels in wild type and *Mif* deficient mice (Figure 3). However, p38 activity was represented as the ratio of phospho-p38 over total p38, and it was increased in fructose-fed WT mice in comparison to WT, while in fructose-fed MIF$^{-/-}$ mice this ratio was increased only in comparison to MIF$^{-/-}$. This is most likely a consequence of attenuated inflammation triggered by *Mif* deletion (Herrero *et al.* 2011). This anti-inflammatory phenotype in fructose-fed *Mif* deficient mice, together with suppressed activation of proinflammatory kinase p38, could set the background for GC action and signaling in VAT (Nikolic *et al.* 2013). Indeed, VAT CORT was elevated in these animals (Figure 4C), most likely as a result of enhanced glucocorticoid prereceptor metabolism, as revealed by elevated 11BHSD1 and H6PDH protein levels in VAT of fructose-fed MIF$^{-/-}$ mice (Figure 4A and B). This result is in

accordance with human and animal studies showing that fructose can elevate 11BHSD1 gene expression in VAT (London & Castonguay 2011), which can further increase visceral adiposity and have deleterious metabolic effects (Walker 2006; Atsumi *et al.* 2007; Nikolic *et al.* 2013). As expected, increased CORT and glucocorticoid prereceptor metabolism in VAT were accompanied with elevated GR protein level (Figure 4D), implying regulatory loop between MIF and GCs in conditions of energy overload.

In the adipose tissue, GCs can modulate both lipogenesis and lipolysis (Wang *et al.* 2012). However, direction of these effects on adipose tissue lipid storage crucially depend on the nutritional and/or hormonal conditions (Kleemann & Bucala 2010; Peckett *et al.* 2011; Saksida *et al.* 2013). Although GCs preferably induce adipose tissue lipolysis, they can increase the expression of numerous genes involved in lipogenesis and fat deposition, acting synergistically with supraphysiological insulin levels [17]. In the present study, the expression of glucocorticoid-positively regulated lipolytic gene *Hsl* was unaffected in fructose-fed $MIF^{-/-}$ mice (Figure 5), which could partly be a consequence of anti-lipolytic activity of increased insulin (Duncan *et al.* 2007). On the other hand, *Atgl* expression in VAT of these animals was increased, but, it was not accompanied with increased plasma FFA release (Table 1). On the basis of increased *Pepck*, known to be involved in FFA re-esterification in the adipose tissue (Zhou *et al.* 2015), we could presume that increased adipose tissue FFA is channeled into triglyceride synthesis instead of being released, resulting in significantly larger adipocytes (Figure 5 and 1). The hypertrophic adipocytes could also be the result of greater triglyceride uptake from circulation (Merkel *et al.* 2002; Wang & Eckel 2009), since both increased VAT *Lpl* gene expression and unaltered triglyceride level were observed in *Mif* deficient mice on fructose diet (Table 1, Figure 5).

In the present study, the main resultant of fructose consumption combined with *Mif* deficiency was the activation of glucocorticoid-regulated enzymes involved in VAT *de novo*

lipogenesis (Figure 5). Namely, the significant increase of *Fas* and *Acc* mRNA levels was observed in VAT of fructose-fed $MIF^{-/-}$ mice, which are both critically involved in *de novo* lipogenesis (Strable & Ntambi 2010). They are under direct expressional control of SREBP1c (Mandard & Kersten 2006), which is known to be regulated by both GCs and insulin (Kim *et al.* 1998; Foretz *et al.* 1999; Ayala-Sumuano *et al.* 2013). Indeed, SREBP1c was significantly increased in the VAT of fructose-fed $MIF^{-/-}$ mice, which was consistent with the observed hypertrophic state of adipocytes (Figures 1 and 6). Yet another transcriptional regulator involved in adipogenesis, PPARG, was also significantly increased in the VAT of the same animals (Figure 6). Previous studies, investigating the role of MIF in adipogenesis, showed that $MIF^{-/-}$ cells had elevated PPARG expression during adipocyte differentiation (Atsumi *et al.* 2007). However, in our study, significant effect on PPARG protein level was observed only when $MIF^{-/-}$ mice were fed with fructose, while it was not changed either in $MIF^{-/-}$ mice on standard diet or in the fructose-fed WT mice, which implies that fructose-rich diet generates both adipogenesis and hypertrophy only in the absence of *Mif*. These results shed a new light on the role of MIF in the diet-induced obesity, where *Mif* deficiency promotes visceral adiposity and has detrimental effects on adipose tissue lipid metabolism under the conditions of energy overload.

In conclusion, the present study showed that *Mif* deficiency is important for development of glucose and insulin resistance. The metabolic stress, in the form of energy-rich fructose diet, led to visceral adiposity and adipocyte hypertrophy in *Mif* deficient mice, concomitantly with stimulated adipose tissue lipogenesis. These harmful effects of *Mif* deficiency are most likely conducted through the enhanced glucocorticoid prereceptor metabolism and facilitated glucocorticoid-regulated lipogenesis in the VAT. Therefore, we propose that a crucial factor for glucocorticoid-mediated adiposity in response to fructose-

enriched diet is the deficiency of *Mif*, whose absence provides the setting of hyperinsulinemia and insulin resistance.

Declaration of Interest

All authors declare that they have no conflicts of interest.

Funding

This work was supported by the Ministry of Education, Science and Technological Development of the Republic of Serbia (Grant No III41009) and by "Start Up for Science" grant from the Center for Leadership Development.

Author contributions

Ljupka Gligorovska conducted the experiments, analyzed the data and wrote the paper. Biljana Bursać provided experimental help, Sanja Kovačević performed hystological anlyses. Nataša Veličković and Gordana Matić revised the paper before submission. Ana Djordjevic designed the study and revised the paper before submission.

Acknowledgement

The authors are thankful to Dr. Stanislava Stošić Grujičić and Dr. Ivana Stojanović for providing $MIF^{-/-}$ animals.

References

Aeberli D, Yang Y, Mansell A, Santos L, Leech M & Morand EF 2006a Endogenous macrophage migration inhibitory factor modulates glucocorticoid sensitivity in macrophages via effects on MAP kinase phosphatase-1 and p38 MAP kinase. *FEBS Letters* **580** 974–981. (doi:10.1016/j.febslet.2006.01.027)

Aeberli D, Leech M & Morand EF 2006b Macrophage migration inhibitory factor and glucocorticoid sensitivity. *Rheumatology* **45** 937–943. (doi:10.1093/rheumatology/kel142)

Atsumi T, Cho Y-R, Leng L, McDonald C, Yu T, Danton C, Hong E-G, Mitchell RA, Metz C, Niwa H *et al.* 2007 The proinflammatory cytokine macrophage migration inhibitory factor regulates glucose metabolism during systemic inflammation. *Journal of Immunology (Baltimore, Md. : 1950)* **179** 5399–5406.

Ayala-Sumuano J-T, Velez-delValle C, Beltrán-Langarica A, Marsch-Moreno M, Hernandez-Mosqueira C & Kuri-Harcuch W 2013 Glucocorticoid Paradoxically Recruits Adipose Progenitors and Impairs Lipid Homeostasis and Glucose Transport in Mature Adipocytes. *Scientific Reports* **3** 2573. (doi:10.1038/srep02573)

Basciano H, Federico L & Adeli K 2005 Fructose, insulin resistance, and metabolic dyslipidemia. *Nutrition & Metabolism* **2** 5. (doi:10.1186/1743-7075-2-5)

Calandra T & Bucala R 1997 Macrophage migration inhibitory factor (MIF): a glucocorticoid counter-regulator within the immune system. *Critical Reviews in Immunology* **17** 77–88.

Calandra T, Bernhagen J, Metz CN, Spiegel LA, Bacher M, Donnelly T, Cerami A & Bucala R 1995 MIF as a glucocorticoid-induced modulator of cytokine production. *Nature* **377**

68–71. (doi:10.1038/377068a0)

Campbell JE, Peckett AJ, D'souza AM, Hawke TJ & Riddell MC 2011 Adipogenic and lipolytic effects of chronic glucocorticoid exposure. *American Journal of Physiology-Cell Physiology* **300** C198–C209. (doi:10.1152/ajpcell.00045.2010)

Chakravarty K, Cassuto H, Reshef L & Hanson RW 2005 Factors That Control the Tissue-Specific Transcription of the Gene for Phosphoenolpyruvate Carboxykinase-C. *Critical Reviews in Biochemistry and Molecular Biology* **40** 129–154. (doi:10.1080/10409230590935479)

Cheng P-W, Lin Y-T, Ho W-Y, Lu P-J, Chen H-H, Lai C-C, Sun G-C, Yeh T-C, Hsiao M, Tseng C-J *et al.* 2017 Fructose induced neurogenic hypertension mediated by overactivation of p38 MAPK to impair insulin signaling transduction caused central insulin resistance. *Free Radical Biology and Medicine* **112** 298–307. (doi:10.1016/j.freeradbiomed.2017.07.022)

Chuang C-C, Martinez K, Xie G, Kennedy A, Bumrungpert A, Overman A, Jia W & McIntosh MK 2010 Quercetin is equally or more effective than resveratrol in attenuating tumor necrosis factor-α–mediated inflammation and insulin resistance in primary human adipocytes. *The American Journal of Clinical Nutrition* **92** 1511–1521. (doi:10.3945/ajcn.2010.29807)

Cvetkovic I, Al-Abed Y, Miljkovic D, Maksimovic-Ivanic D, Roth J, Bacher M, Lan HY, Nicoletti F & Stosic-Grujicic S 2005 Critical Role of Macrophage Migration Inhibitory Factor Activity in Experimental Autoimmune Diabetes. *Endocrinology* **146** 2942–2951. (doi:10.1210/en.2004-1393)

Duncan RE, Ahmadian M, Jaworski K, Sarkadi-Nagy E & Sul HS 2007 Regulation of

Lipolysis in Adipocytes. *Annual Review of Nutrition* **27** 79–101. (doi:10.1146/annurev.nutr.27.061406.093734)

Eberlé D, Hegarty B, Bossard P, Ferré P & Foufelle F 2004 SREBP transcription factors: Master regulators of lipid homeostasis. *Biochimie* **86** 839–848. (doi:10.1016/j.biochi.2004.09.018)

Fingerle-Rowson G, Petrenko O, Metz CN, Forsthuber TG, Mitchell R, Huss R, Moll U, Muller W & Bucala R 2003 The p53-dependent effects of macrophage migration inhibitory factor revealed by gene targeting. *Proceedings of the National Academy of Sciences* **100** 9354–9359. (doi:10.1073/pnas.1533295100)

Finucane OM, Reynolds CM, McGillicuddy FC, Harford KA, Morrison M, Baugh J & Roche HM 2014 Macrophage migration inhibitory factor deficiency ameliorates high-fat diet induced insulin resistance in mice with reduced adipose inflammation and hepatic steatosis. *PLoS ONE* **9** 1–14. (doi:10.1371/journal.pone.0113369)

Foretz M, Guichard C, Ferré P & Foufelle F 1999 Sterol regulatory element binding protein-1c is a major mediator of insulin action on the hepatic expression of glucokinase and lipogenesis-related genes. *Proceedings of the National Academy of Sciences of the United States of America* **96** 12737–12742.

Galarraga M, Campión J, Muñoz-Barrutia A, Boqué N, Moreno H, Martínez JA, Milagro F & Ortiz-de-Solórzano C 2012 Adiposoft: automated software for the analysis of white adipose tissue cellularity in histological sections. *Journal of Lipid Research* **53** 2791–2796. (doi:10.1194/jlr.D023788)

Heinrichs D, Berres M-L, Coeuru M, Knauel M, Nellen A, Fischer P, Philippeit C, Bucala R, Trautwein C, Wasmuth HE *et al.* 2014 Protective role of macrophage migration

inhibitory factor in nonalcoholic steatohepatitis. *The FASEB Journal* **28** 5136–5147. (doi:10.1096/fj.14-256776)

Herrero LJ, Nelson M, Srikiatkhachorn A, Gu R, Anantapreecha S, Fingerle-Rowson G, Bucala R, Morand E, Santos LL & Mahalingam S 2011 Critical role for macrophage migration inhibitory factor (MIF) in Ross River virus-induced arthritis and myositis. *Proceedings of the National Academy of Sciences of the United States of America* **108** 12048–12053. (doi:10.1073/pnas.1101089108)

Kim JB, Sarraf P, Wright M, Yao KM, Mueller E, Solanes G, Lowell BB & Spiegelman BM 1998 Nutritional and insulin regulation of fatty acid synthetase and leptin gene expression through ADD1/SREBP1. *Journal of Clinical Investigation* **101** 1–9. (doi:10.1172/JCI1411)

Kim B-S, Pallua N, Bernhagen J & Bucala R 2015 The macrophage migration inhibitory factor protein superfamily in obesity and wound repair. *Experimental & Molecular Medicine* **47** e161. (doi:10.1038/emm.2015.26)

Kleemann R & Bucala R 2010 Macrophage migration inhibitory factor: critical role in obesity, insulin resistance, and associated comorbidities. *Mediators of Inflammation* **2010** 610479. (doi:10.1155/2010/610479)

Kovačević S, Nestorov J, Matić G & Elaković I 2016 Fructose and stress induce opposite effects on lipid metabolism in the visceral adipose tissue of adult female rats through glucocorticoid action. *European Journal of Nutrition* 1–14. (doi:10.1007/s00394-016-1251-8)

Lee M-J, Pramyothin P, Karastergiou K & Fried SK 2014 Deconstructing the roles of glucocorticoids in adipose tissue biology and the development of central obesity.

536 *Biochimica et Biophysica Acta* **1842** 473–481. (doi:10.1016/j.bbadis.2013.05.029)

537 London E & Castonguay TW 2011 High fructose diets increase 11β-hydroxysteroid
538 dehydrogenase type 1 in liver and visceral adipose in rats within 24-h exposure. *Obesity*
539 *(Silver Spring, Md.)* **19** 925–932. (doi:10.1038/oby.2010.284)

540 Lowry OH, Rosebrough NJ, Farr AL & Randall RJ 1951 PROTEIN MEASUREMENT
541 WITH THE FOLIN PHENOL REAGENT. *Journal of Biological Chemistry* **193** 265–
542 275.

543 Mandard S & Kersten S 2006 Regulation of Lipogenic Genes in Obesity. In *Nutritional*
544 *Genomics*, pp 208–219. Weinheim, FRG: Wiley-VCH Verlag GmbH & Co. KGaA.
545 (doi:10.1002/3527608109.ch12)

546 Mariniello B, Ronconi V, Rilli S, Bernante P, Boscaro M, Mantero F & Giacchetti G 2006
547 Adipose tissue 11beta-hydroxysteroid dehydrogenase type 1 expression in obesity and
548 Cushing's syndrome. *European Journal of Endocrinology* **155** 435–441.
549 (doi:10.1530/eje.1.02228)

550 Merkel M, Eckel RH & Goldberg IJ 2002 Lipoprotein lipase: genetics, lipid uptake, and
551 regulation. *Journal of Lipid Research* **43** 1997–2006.

552 Monteiro R & Azevedo I 2010 Chronic inflammation in obesity and the metabolic syndrome.
553 *Mediators of Inflammation* **2010**. (doi:10.1155/2010/289645)

554 Morrison MC & Kleemann R 2015 Role of Macrophage Migration Inhibitory Factor in
555 Obesity, Insulin Resistance, Type 2 Diabetes, and Associated Hepatic Co-Morbidities: A
556 Comprehensive Review of Human and Rodent Studies. *Frontiers in Immunology* **6**.
557 (doi:10.3389/fimmu.2015.00308)

Nikolic I, Vujicic M, Saksida T, Berki T, Stosic-Grujicic S & Stojanovic I 2013 The role of endogenous glucocorticoids in glucose metabolism and immune status of MIF-deficient mice. *Archives of Biological Sciences* **714** 499–505. (doi:10.1016/j.ejphar.2013.06.037)

Peckett AJ, Wright DC & Riddell MC 2011 The effects of glucocorticoids on adipose tissue lipid metabolism. *Metabolism* **60** 1500–1510. (doi:10.1016/j.metabol.2011.06.012)

Pektas MB, Koca HB, Sadi G & Akar F 2016 Dietary Fructose Activates Insulin Signaling and Inflammation in Adipose Tissue: Modulatory Role of Resveratrol. *BioMed Research International* **2016** 1–10. (doi:10.1155/2016/8014252)

Rosen ED & Spiegelman BM 2001 PPARγ: a Nuclear Regulator of Metabolism, Differentiation, and Cell Growth. *Journal of Biological Chemistry* **276** 37731–37734. (doi:10.1074/jbc.R100034200)

Sakaue S, Nishihira J, Hirokawa J, Yoshimura H, Honda T, Aoki K, Tagami S & Kawakami Y 1999 Regulation of macrophage migration inhibitory factor (MIF) expression by glucose and insulin in adipocytes in vitro. *Molecular Medicine (Cambridge, Mass.)* **5** 361–371.

Saksida T, Stosic-Grujicic S & Stojanovic I 2013 The role of macrophage migration inhibitory factor in obesity-associated type 2 diabetes in mice. *Archives of Biological Sciences* **65** 499–505. (doi:10.2298/ABS1302499S)

Seckl JR, Morton NM, Chapman KE & Walker BR 2004 Glucocorticoids and 11beta-hydroxysteroid dehydrogenase in adipose tissue. *Recent Progress in Hormone Research* **59** 359–393.

Serre-Beinier V, Toso C, Morel P, Gonelle-Gispert C, Veyrat-Durebex C, Rohner-Jeanrenaud

F, Calandra T, Roger T, James RW, Montet X *et al.* 2010 Macrophage migration inhibitory factor deficiency leads to age-dependent impairment of glucose homeostasis in mice. *The Journal of Endocrinology* **206** 297–306. (doi:10.1677/JOE-09-0342)

Strable MS & Ntambi JM 2010 Genetic control of de novo lipogenesis: role in diet-induced obesity. *Critical Reviews in Biochemistry and Molecular Biology* **45** 199–214. (doi:10.3109/10409231003667500)

Tappy L & Le K-A 2010 Metabolic Effects of Fructose and the Worldwide Increase in Obesity. *Physiological Reviews* **90** 23–46. (doi:10.1152/physrev.00019.2009)

Vazquez Prieto MA, Bettaieb A, Rodriguez Lanzi C, Soto VC, Perdicaro DJ, Galmarini CR, Haj FG, Miatello RM & Oteiza PI 2015 Catechin and quercetin attenuate adipose inflammation in fructose-fed rats and 3T3-L1 adipocytes. *Molecular Nutrition & Food Research* **59** 622–633. (doi:10.1002/mnfr.201400631)

Veličković N, Djordjevic A, Vasiljević A, Bursać B, Milutinović DV & Matić G 2013 Tissue-specific regulation of inflammation by macrophage migration inhibitory factor and glucocorticoids in fructose-fed Wistar rats. *British Journal of Nutrition* **110** 456–465. (doi:10.1017/S0007114512005193)

Verschuren L, Kooistra T, Bernhagen J, Voshol PJ, Ouwens DM, van Erk M, de Vries-van der Weij J, Leng L, van Bockel JH, van Dijk KW *et al.* 2009 MIF deficiency reduces chronic inflammation in white adipose tissue and impairs the development of insulin resistance, glucose intolerance, and associated atherosclerotic disease. *Circulation Research* **105** 99–107. (doi:10.1161/CIRCRESAHA.109.199166)

Walker BR 2006 Cortisol?cause and cure for metabolic syndrome? *Diabetic Medicine* **23** 1281–1288. (doi:10.1111/j.1464-5491.2006.01998.x)

603 Wang H & Eckel RH 2009 Lipoprotein lipase: from gene to obesity. *American Journal of*
604 *Physiology-Endocrinology and Metabolism* **297** E271–E288.
605 (doi:10.1152/ajpendo.90920.2008)

606 Wang J-C, Gray NE, Kuo T & Harris CA 2012 Regulation of triglyceride metabolism by
607 glucocorticoid receptor. *Cell & Bioscience* **2** 19. (doi:10.1186/2045-3701-2-19)

608 Zhou D, Wang H, Cui H, Chen H & Pan Y-X 2015 Early-life exposure to high-fat diet may
609 predispose rats to gender-specific hepatic fat accumulation by programming Pepck
610 expression. *The Journal of Nutritional Biochemistry* **26** 433–440.
611 (doi:10.1016/j.jnutbio.2014.10.009)

612

613

614 **Figure captions**

615

616 **Figure 1. Body mass, VAT mass and histological analysis.** Data for body mass and weight
617 gain (**A**), VAT mass (**B**) and VAT/body mass ratio (**C**) are presented as mean ± SD (n = 12
618 animals per group). Representative hematoxylin-eosin staining of VAT sections from
619 C57BL/6J mice (WT) (**D**), WT mice on fructose diet (WT FrD) (**E**), mice with genetically
620 deleted *Mif* ($MIF^{-/-}$) (**F**) and $MIF^{-/-}$ mice on fructose diet ($MIF^{-/-}$ FrD) (**G**) (magnification ×20,
621 bar = 100 μm). Morphometric data on adipocyte cell diameter (**H**) and area (**I**) are presented
622 as mean ± SEM (100 adipocytes per section, three sections per animal and six animals per
623 group). A value of $p < 0.05$ was considered statistically significant. Two-way ANOVA
624 showed significant effect of fructose on VAT mass ($p < 0.01$), VAT/body mass ratio ($p <$
625 0.05), as well as on the adipocyte cell diameter and area ($p < 0.01$). *Mif* deficiency also had
626 significant effect on both VAT and VAT/body mass ratio ($p < 0.001$), as well as on the
627 adipocyte cell diameter ($p < 0.01$) and area ($p < 0.05$). Significant between-group differences
628 from *post hoc* Tukey test are given as follows: $^{*}p < 0.05$, $^{**}p < 0.01$, $^{***}p < 0.001$, all groups
629 *vs.* WT; $^{\#}p < 0.05$, $^{\#\#}p < 0.01$, $MIF^{-/-}$ FrD *vs.* WT FrD; $^{\dagger}p < 0.05$, $MIF^{-/-}$ FrD *vs.* $MIF^{-/-}$.

630

631 **Figure 2. Intraperitoneal tests of glucose and insulin tolerance (IP-GTT and IP-ITT).**
632 After determination of fasting glucose concentrations, animals were challenged with
633 intraperitoneal injection of glucose (2 g/kg) or insulin (0.75 IU/kg). Blood glucose was
634 measured 15, 30, 60, 90, and 120 minutes after injection, and glucose concentration *vs.* time
635 was plotted for C57BL/6J mice (WT), WT mice on fructose diet (WT FrD), mice with
636 genetically deleted *Mif* ($MIF^{-/-}$) and $MIF^{-/-}$ mice on fructose diet ($MIF^{-/-}$ FrD). A value of $p <$
637 0.05 was considered statistically significant. Data are presented as mean ± SD (n = 12
638 animals per group). Significant between-group differences from *post hoc* Tukey test are given

as follows: $^{*}p < 0.05$, $^{**}p < 0.01$, $^{***}p < 0.001$, all groups *vs.* WT; $^{\#}p < 0.05$, $^{\#\#}p < 0.01$, $^{\#\#\#}p < 0.001$, MIF$^{-/-}$ FrD *vs.* WT FrD; $^{\dagger}p < 0.05$, MIF$^{-/-}$ FrD *vs.* MIF$^{-/-}$.

Figure 3. Phosphorylated and total p38 kinase and their ratio in the VAT. Representative Western blots and relative quantification of total and phospho-p38 kinase and their ratio in the total protein extract of VAT from C57BL/6J mice (WT), WT mice on fructose diet (WT FrD), mice with genetically deleted *Mif* (MIF$^{-/-}$) and MIF$^{-/-}$ mice on fructose diet (MIF$^{-/-}$ FrD). Immunoreactivities of total and phosphorylated p38 are normalized to Beta-actin as loading control and the data are presented as mean ± SEM (n = 12 animals per group). A value of $p < 0.05$ was considered statistically significant. Two-way ANOVA showed that total p38 protein level was significantly affected by *Mif* deficiency ($p < 0.001$) and its interaction with fructose diet ($p < 0.001$). Phosphorylation and activity of p38 was significantly affected only by fructose ($p < 0.001$). Significant between-group differences from *post hoc* Tukey test are given as follows: $^{*}p < 0.05$, $^{***}p < 0.001$, all groups *vs.* WT; $^{\#\#\#}p < 0.001$, MIF$^{-/-}$ FrD *vs.* WT FrD; $^{\dagger}p < 0.05$; $^{\dagger}p < 0.05$, $^{\dagger\dagger\dagger}p < 0.001$, MIF$^{-/-}$ FrD *vs.* MIF$^{-/-}$.

Figure 4. Glucocorticoid prereceptor metabolism and signaling. Representative Western blots and relative quantification of 11βHSD1 (**A**), H6PDH (**B**) and GR (**D**) protein levels and CORT concentration (**C**) in total protein extract of VAT from C57BL/6J mice (WT), WT mice on fructose diet (WT FrD), mice with genetically deleted *Mif* (MIF$^{-/-}$) and MIF$^{-/-}$ mice on fructose diet (MIF$^{-/-}$ FrD). Immunoreactivities of 11βHSD1, H6PDH and GR (normalized to Beta-actin as loading control) are expressed as mean ± SEM, while the results for VAT CORT concentration are presented as mean ± SD (n = 12 animals per group). A value of $p < 0.05$ was considered statistically significant. Two-way ANOVA showed significant effects of fructose ($p < 0.01$) and *Mif* deficiency ($p < 0.05$) for both 11βHSD1 and H6PDH protein

664 level, while GR was affected only by fructose treatment ($p < 0.01$). CORT concentration in
665 VAT was affected by fructose diet ($p < 0.05$), as well as by its interaction with *Mif* deficiency
666 ($p < 0.05$). Significant between-group differences from *post hoc* Tukey test are given as
667 follows: $^{*}p < 0.05$, $^{**}p < 0.01$, $^{***}p < 0.001$, all groups *vs.* WT; $^{\#}p < 0.05$, MIF$^{-/-}$ FrD *vs.* WT
668 FrD; $^{\dagger\dagger}p < 0.01$, MIF$^{-/-}$ FrD *vs.* MIF$^{-/-}$.
669
670 **Figure 5. Relative levels of mRNA for genes involved in VAT lipid metabolism.** Relative
671 quantification of *Hsl, Atgl, Pepck, Lpl, Acc and Fas* mRNA level, normalized to *Hprt1*
672 housekeeping gene, in the VAT of C57BL/6J mice (WT), WT mice on fructose diet (WT
673 FrD), mice with genetically deleted *Mif* (MIF$^{-/-}$) and MIF$^{-/-}$ mice on fructose diet (MIF$^{-/-}$ FrD).
674 Data are presented as mean ± SEM (n = 12 animals per group) of the triplicate analysis of
675 RNA samples. A value of $p < 0.05$ was considered statistically significant. According to two-
676 way ANOVA the effect of fructose was detected for *Atgl* ($p < 0.01$), *Pepck* ($p < 0.001$), *Fas*
677 ($p < 0.05$) and *Acc* ($p < 0.01$) mRNA levels. *Mif* deficiency significantly affected expression
678 of *Atgl* ($p < 0.01$), *Pepck* ($p < 0.001$), *Lpl* ($p < 0.001$), *Fas* ($p < 0.01$) and *Acc* ($p < 0.01$).
679 Interaction between fructose and the absence of MIF was detected for *Atgl* ($p < 0.05$), *Pepck*
680 ($p < 0.001$), *Lpl* ($p < 0.001$), *Fas* ($p < 0.05$) and *Acc* ($p < 0.05$) mRNA levels. Significant
681 between-group differences from *post hoc* Tukey test are given as follows: $^{*}p < 0.05$, $^{**}p <$
682 0.01, $^{***}p < 0.001$, all groups *vs.* WT; $^{\#\#}p < 0.01$, $^{\#\#\#}p < 0.001$, MIF$^{-/-}$ FrD *vs.* WT FrD; $^{\dagger}p <$
683 0.05, $^{\dagger\dagger}p < 0.01$, MIF$^{-/-}$ FrD *vs.* MIF$^{-/-}$.
684
685 **Figure 6. Transcriptional regulators of VAT lipid metabolism.** Representative Western
686 blots and relative quantification of PPARG (**A**) and SREBP1c (**B**) total protein levels in the
687 VAT of C57BL/6J mice (WT), WT mice on fructose diet (WT FrD), mice with genetically
688 deleted *Mif* (MIF$^{-/-}$) and MIF$^{-/-}$ mice on fructose diet (MIF$^{-/-}$ FrD). Beta-actin was used as a

loading control. Data are presented as mean ± SEM (n = 12 animals per group). A value of $p < 0.05$ was considered statistically significant. Two-way ANOVA showed significant effects of fructose diet on both PPARG ($p < 0.01$) and SREBP1c ($p < 0.001$), while the deficiency of *Mif* affected only SREBP1c protein level ($p < 0.01$). Between-group differences from *post hoc* Tukey test are given as follows: $^{*}p < 0.05$, $^{***}p < 0.001$, all groups *vs.* WT; $^{\#\#}p < 0.01$, MIF$^{-/-}$ FrD *vs.* WT FrD; $^{\dagger}p < 0.05$, $^{\dagger\dagger}p < 0.01$, MIF$^{-/-}$ FrD *vs.* MIF$^{-/-}$.

Table 1. Physiological and biochemical parameters: food, liquid and energy intake, triglycerides and FFA

	WT	WT FrD	MIF$^{-/-}$	MIF$^{-/-}$ FrD	Two-way ANOVA		
					Fructose	*Mif* deficiency	Interaction
Food intake (g/day/animal)	9.30 ± 2.0	5.76 ± 1.33***	8.79 ± 1.46	5.59 ± 1.20***†††	< 0.001	NS	NS
Liquid intake (ml/day/animal)	11.91 ± 2.79	16.86 ± 3.07***	10.88 ± 2.15	14.96 ± 2.66$^{***\#\#\#\dagger\dagger\dagger}$	< 0.001	< 0.001	NS
Energy intake (kJ/day/animal)	102.35 ± 22.03	129.20 ± 18.86***	100.76 ± 14.79	117.98 ± 20.89$^{***\#\dagger\dagger\dagger}$	< 0.01	< 0.05	NS
Triglycerides (mmol/l)	0.93±0.15	1.16±0.32	1.21±0.37	1.24±0.43	NS	NS	NS
FFA (mmol/l)	1.83±0.45	1.78±0.43	2.03±0.47	1.94±0.44	NS	NS	NS

The data are presented as means ± SD (n = 12 animals per group). A value of $p < 0.05$ was considered statistically significant. Significant between-groups differences obtained from two-way ANOVA followed by *post hoc* Tukey test are given as follows:

$^{***}p < 0.001$, all groups *vs.* WT

$^{\#}p < 0.05$; $^{\#\#}p < 0.01$; $^{\#\#\#}p < 0.001$, MIF$^{-/-}$ FrD *vs.* WT FrD

$^{\dagger}p < 0.05$; $^{\dagger\dagger\dagger}p < 0.001$, MIF$^{-/-}$ FrD *vs.* MIF$^{-/-}$

FrD: fructose diet; NS: not significant

Table 2. Insulin sensitivity parameters: fasting glucose, insulin, IP-GTT glucose AUC and IP-ITT glucose AUC

	WT	WT FrD	MIF$^{-/-}$	MIF$^{-/-}$ FrD	Two-way ANOVA		
					Fructose	*Mif* deficiency	Interaction
Glucose (mmol/l)	5.04 ± 0.72	4.53 ± 0.92	5.92 ± 0.42*	5.52 ± 0.68$^{\#\#}$	< 0.05	< 0.001	NS
Insulin (mmol/l)	1.68 ± 0.51	2.94 ± 1.83	6.28 ± 2.14*	8.09 ± 7.57$^{**\#}$	< 0.01	< 0.05	NS
IP-GTT glucose AUC	1603.13 ± 77.58	1906.31 ± 146.86	2199.00 ± 370.11***	2626.50 ± 178.71$^{***\#\#\#\dagger}$	< 0.01	< 0.001	NS
IP-ITT glucose AUC	618.90 ± 60.73	624.75 ± 66.96	924.88 ± 62.83***	869.25 ± 110.83$^{***\#\#\#}$	NS	< 0.001	NS

The data are presented as means ± SD (n = 12 animals per group). A value of $p < 0.05$ was considered statistically significant. Significant between-groups differences obtained from two-way ANOVA followed by *post hoc* Tukey test are given as follows:

$^{*}p < 0.05$; $^{**}p < 0.01$, all groups *vs.* WT

$^{\#}p < 0.05$; $^{\#\#}p < 0.01$; $^{\#\#\#}p < 0.001$, MIF$^{-/-}$ FRD *vs.* WT FRD

$^{\dagger}p < 0.05$, MIF$^{-/-}$ FRD *vs.* MIF$^{-/-}$

FrD: fructose diet; NS: not significant

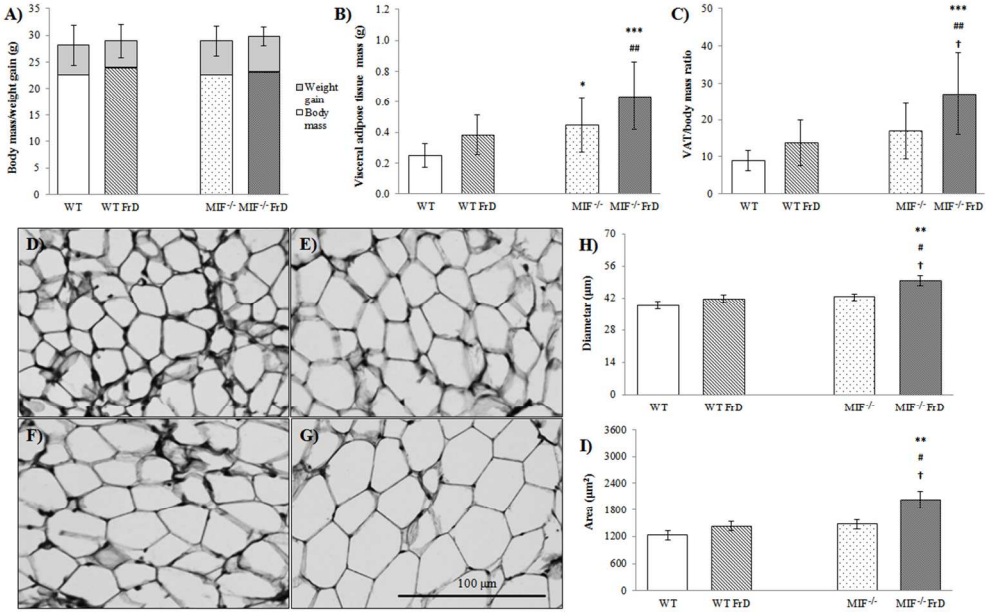

Figure 1

418x257mm (72 x 72 DPI)

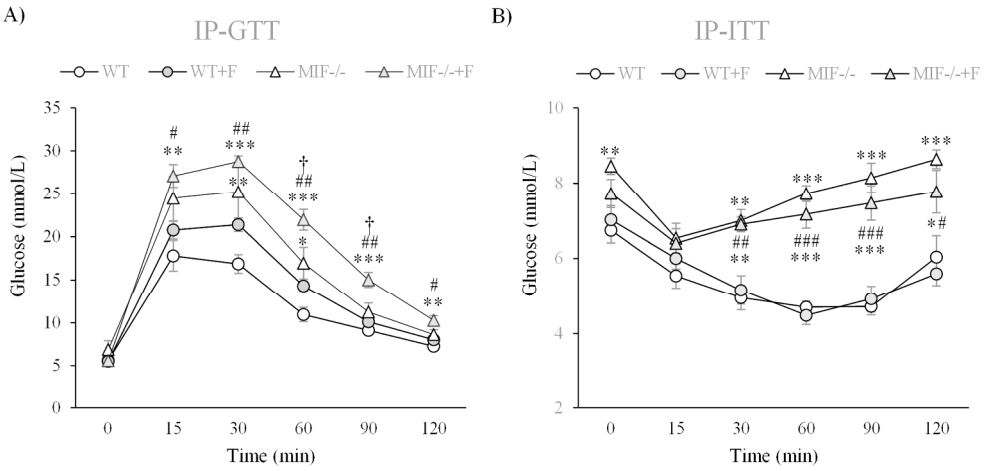

Figure 2

181x90mm (300 x 300 DPI)

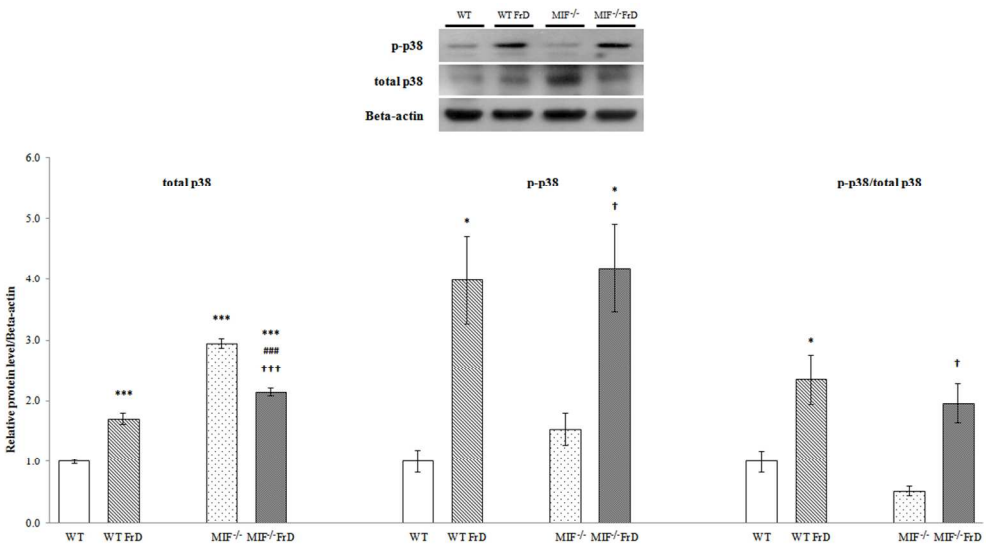

Figure 3

408x224mm (72 x 72 DPI)

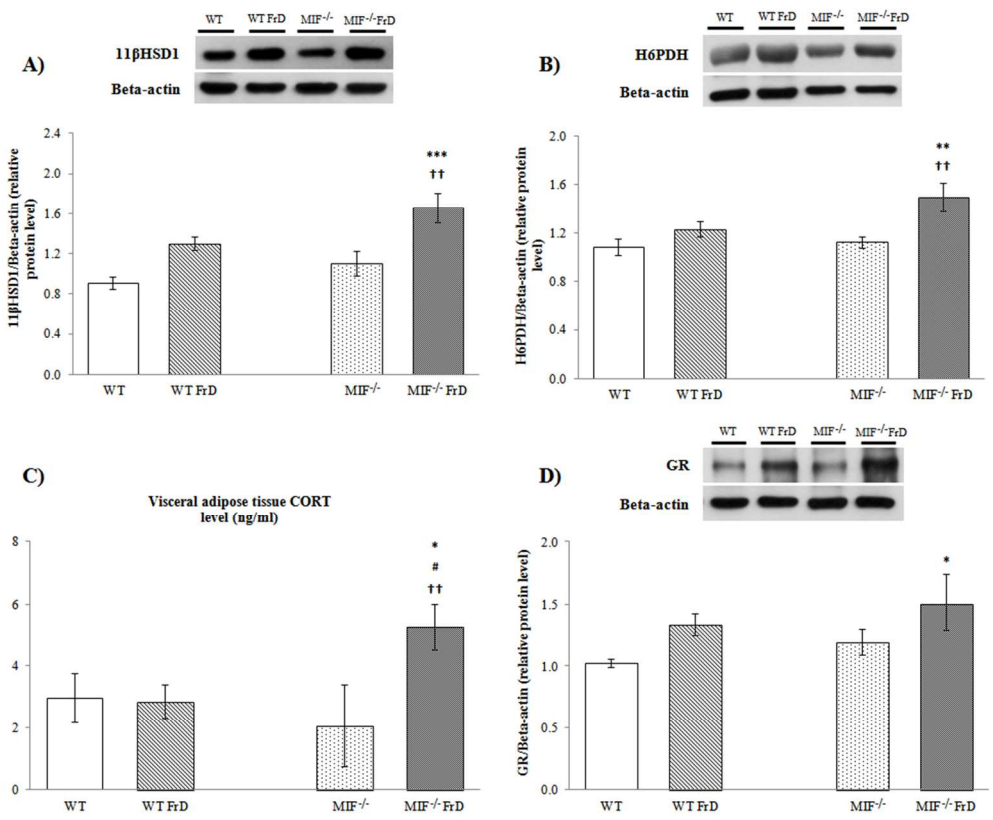

Figure 4

344x281mm (72 x 72 DPI)

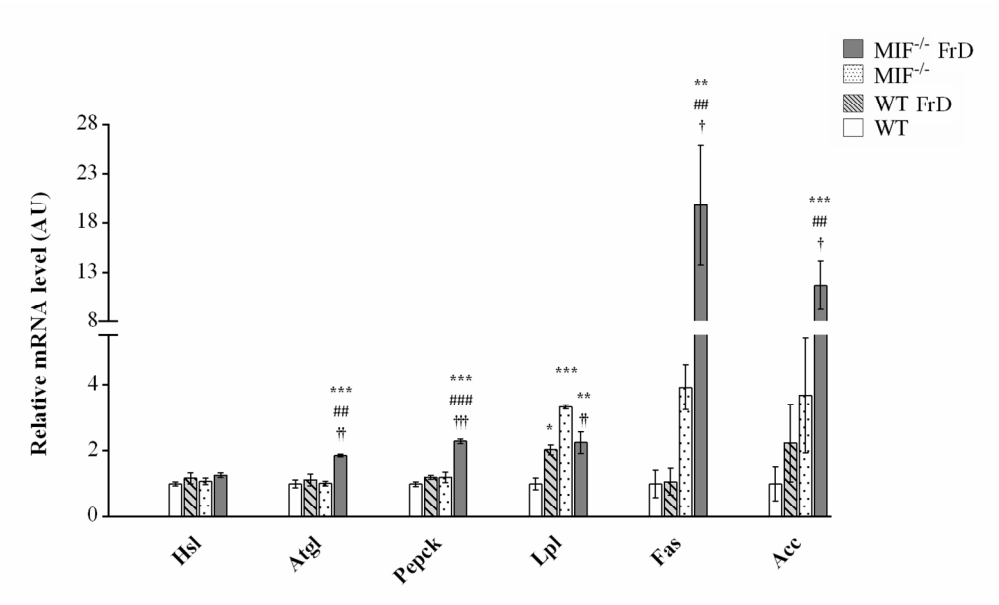

Figure 5

129x78mm (300 x 300 DPI)

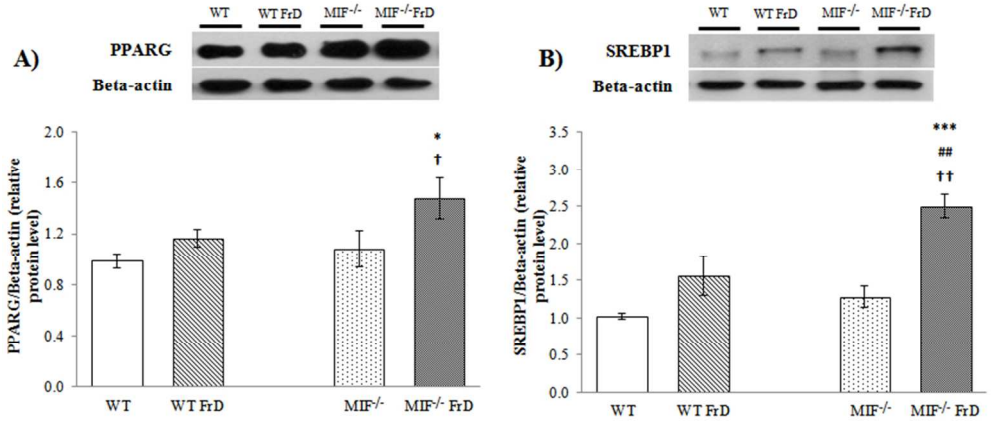

Figure 6

298x129mm (72 x 72 DPI)